Neutrophil extracellular traps mediate transfer of cytoplasmic neutrophil antigens to myeloid dendritic cells toward ANCA induction and associated autoimmunity

*Sabina Sangaletti,[1] *Claudio Tripodo,[2] Claudia Chiodoni,[1] Carla Guarnotta,[2] Barbara Cappetti,[1] Patrizia Casalini,[3] Silvia Piconese,[1] Mariella Parenza,[1] Cristiana Guiducci,[4] Caterina Vitali,[1] and Mario P. Colombo[1]

[1]Molecular Immunology Unit, Department of Experimental Oncology and Molecular Medicine, Fondazione Istituti di Ricovero e Cura a Carattere Scientifico Istituto Nazionale Tumori, Milan, Italy; [2]Department of Human Pathology, University of Palermo, Palermo, Italy; [3]Molecular Targeting Unit, Department of Experimental Oncology and Molecular Medicine, Fondazione Istituti di Ricovero e Cura a Carattere Scientifico Istituto Nazionale Tumori, Milan, Italy; and [4]Dynavax Technologies Corporation, Berkeley, CA

Antineutrophil cytoplasmic antibodies (ANCAs) target proteins normally retained within neutrophils, indicating that cell death is involved in the autoimmunity process. Still, ANCA pathogenesis remains obscure. ANCAs activate neutrophils inducing their respiratory burst and a peculiar form of cell death, named NETosis, characterized by formation of neutrophil extracellular traps (NETs), decondensed chromatin threads decorated with cytoplasmic proteins endorsed with antimicrobial activity. NETs have been consistently detected in ANCA-associated small-vessel vasculitis, and this association prompted us to test whether the peculiar structure of NET favors neutrophil proteins uploading into myeloid dendritic cells and the induction of ANCAs and associated autoimmunity. Here we show that myeloid DCs uploaded with and activated by NET components induce ANCA and autoimmunity when injected into naive mice. DC uploading and autoimmunity induction are prevented by NET treatment with DNAse, indicating that NET structural integrity is needed to maintain the antigenicity of cytoplasmic proteins. We found NET intermingling with myeloid dendritic cells also positive for neutrophil myeloperoxidase in myeloperoxidase-ANCA-associated microscopic poliangiitis providing a potential correlative picture in human pathology. These data provide the first demonstration that NET structures are highly immunogenic such to trigger adaptive immune response relevant for autoimmunity. (*Blood*. 2012; 120(15):3007-3018)

Introduction

Polymorphonuclear leukocytes (PMNs) are harnessed to attack invading pathogens through a variety of antimicrobial peptides and enzymes but are also capable of regulatory functions toward many aspects of innate responses.[1] Less established is their participation to adaptive immune responses, although they take part to the effector phase of anticancer immunity and autoimmunity.[2,3]

A peculiar feature of PMN is their extrusion of neutrophil extracellular traps (NETs), structures of decondensed chromatin decorated with antimicrobial peptides, such as myeloperoxidase (MPO), elastase, proteinase 3 (PR3), cathepsin G, lactoferrin, and others. Like a bee that dies losing its sting, PMNs extrude NET while dying to trap bacteria.[4] Accordingly, this type of cell death, which is distinct from necrosis or apoptosis,[5] has been also defined antimicrobial cell death.[6] The contribution of PMNs, and specifically of NETs, to autoimmunity has gathered ever-increasing attention. Specific neutrophil-[7] and granulopoiesis-related[8] signatures have been identified in patients with antineutrophil cytoplasmic antibody (ANCA)–related autoimmunity and systemic lupus erythematosus (SLE), respectively, and NET formation has been observed in these pathologic autoimmune settings. Neutrophils from SLE patients, chronically activated by autoantibodies, release NETs that induce plasmacytoid dendritic cells (pDCs) to secrete IFN-α toward exacerbation of the autoimmune process.[9-11]

In the renal parenchyma of patients affected by systemic autoimmune small-vessel vasculitis (SVV),[12] NETs have been shown to actively participate to the endothelial damage engendered by ANCA. Thus, there is a close bidirectional relationship between ANCA and NET in autoimmune settings, through which pathogenic ANCA prompt NET formation in turn contributing to the parenchymal damage. Although the pathogenic role of ANCA has been described in different pathologic contexts, little is known about ANCA development. The knowledge that patients' ANCA directed against MPO and PR3 neutrophil proteins recognize conformational epitopes[13,14] suggests that the break of tolerance to these antigens should occur in a context requiring antigen structural and functional integrity. NETs might represent a suitable context for the loss of tolerance toward ANCA targets, being the cytoplasmic antimicrobial proteins associated with NET chromatin threads preserved structurally and functionally. This could be true also in the SLE pathologic setting, in which Lande et al have identified high levels of serum immunogenic complexes composed of neutrophil-derived antimicrobial peptides and self-DNA prompting the idea that such complexes could derive from NET and serve as autoantigens to trigger B-cell activation.[9]

Herein we evaluated whether NET can serve as active vehicles to transfer neutrophil autoantigens to DCs. To this aim, we investigated the effects of the in vitro interaction between myeloid DCs (mDCs) and neutrophils undergoing NETosis and evaluated the outcome of in vivo immunization with mDCs that interacted with NETotic PMN.

Submitted March 8, 2012; accepted August 12, 2012. Prepublished online as *Blood* First Edition paper, August 29, 2012; DOI 10.1182/blood-2012-03-416156.

*S.S. and C.T. contributed equally to this study.

The online version of this article contains a data supplement.

The publication costs of this article were defrayed in part by page charge payment. Therefore, and solely to indicate this fact, this article is hereby marked "advertisement" in accordance with 18 USC section 1734.

Methods

Animals and in vivo treatments

Female BALB/cAnNCr and C57BL/6N mice, 8-10 weeks old, were purchased from Charles River. TNF KO (B6;129S-Tnftm1Gkl/J), IL-6 KO (B6.129S2-Il6tm1Kopf/J), and IFNγ KO [C.129S7(B6)–Ifngtm1Ts/J] were from The Jackson Laboratory. Animals were maintained in filtered top cages at the Istituto Nazionale Tumori. All procedures involving animals were approved by the Institute Ethical Committee and performed in accordance to institutional guidelines and national law (DL116/92), as well as the Declaration of Helsinki.

PMN isolation

Subcutaneously elicited PMNs were collected from blocks of 2% agarose and 0.2% gelatin in saline 5 days after subcutaneous implant by washing 3 times agar blocks with IMDM supplemented with 10% of FCS (GIBCO, Life Technologies). A total of 70%-75% of these cells are PMNs that are enriched up to the 95% after 30 minutes of adherence on plastics.[15] In some cases, naive PMNs were obtained through immunomagnetic cell separation from spleen cells suspension using a specific kit (anti-Ly6G MicroBead Kit, Miltenyi).

NET detection and quantification

To evaluate NET formation, subcutaneously elicited PMNs were seeded onto poly-D-lysine–coated glasses 2 hours or overnight in the presence of the DNA dye SYTOX green (Invitrogen) or of a polyclonal Ab to histones (pan Histones, Chemicon Temecula) conjugated with AlexaFluor-488 dye (labeling kit for mouse IgG); fixed with 2% paraformaldehyde (PFA) and stained with mAbs for MPO (goat polyclonal), PR3 (goat polyclonal), or elastase (rabbit polyclonal), all from Santa Cruz Biotechnology. NETs were evaluated and counted under a microscope. To induce NETosis, naive PMNs were treated with phorbol 12-myristate 13-acetate (PMA; from 20-80nM) in IMDM 2% FCS.

Generation of mDCs from BM precursors

Bone marrow cells were resuspended at 2×10^6 cells/mL in cRPMI 1640 (Invitrogen) supplemented with 5 ng/mL of rGM-CSF and 10 ng/mL of murine rIL-4 (Endogen). On day 3 and 5 of culture, half of the medium was replaced with fresh medium containing GM-CSF and IL-4. On day 7, loosely adherent cells were harvested by gentle pipetting and mDCs were purified with CD11c MiniMacs columns according to the manufacturer's instructions (Miltenyi Biotec). Phenotype of the purified $CD11c^+$ fraction was analyzed by flow cytometry using Abs to CD11c, CD11b, CD45RA, CD40, H-$2K^d$, and I-A^d/I-E^d. According to the nomenclature of dentritic cells,[16] $CD11c^+$, $CD11b^+$, and $CD45RA^-$ cells are referred to as mDCs thereafter. For in vivo migration, mDCs were incubated with green-latex (LX)-microspheres (1:100, DC: microspheres; Fluoresbrite, Polysciences Inc) for 30 minutes at 37°C, and uptake of the LX-microspheres was determined by FACS analysis of CD11c-gated cells following our published procedures.[17] LX microspheres-loaded DCs were then cocultured with PMNs or treated with CpG (5 mg/mL) o/n and injected (2×10^6 cells) intraperitoneally into mice that were killed 48 hours after injection, draining lymph nodes collected and cells analyzed by FACS.

DC-PMN coculture for live cell imaging experiments

PMNs (2×10^5) were seeded onto poly-D-lysine–coated tissue culture dishes (35 mm) specific for immunofluorescence and confocal microscopy (FuoroDish, Word Precision Instruments, Inc) and allowed to adhere for 2 hours in the presence of the DNA SYTOXgreen dye (1:5000, Invitrogen), which stains only the dsDNA of NETotic cells and is excluded from live cells, and Draq5 that stains both the nuclei of live cells and NETs. Medium was replaced before adding 2×10^5 DCs in IMDM 2%. DCs were stained with the vital membrane dye PKH-26 (Sigma-Aldrich) according to the manufacturer's instructions. NET formation and DC-NET/PMN interaction were observed by live cell imaging performed on a BioRad laser scanner confocal (Microradiance 2000) using a × 20, 0.5 NA Plan-Fluor DIC dry objective. The microscope (NIKON TE300 ECLIPSE) was equipped with incubation chamber, which provided a humidified atmosphere at 37°C with 5% CO_2.

Imaging of NET protein transfer to mDCs

To assess the transfer of NET-associated proteins (MPO, PR3) to mDCs, subcutaneously elicited PMNs were cocultured with DCs (stained PKH-26 dye) onto poly-D-lysine–coated glasses in IMDM supplemented with 2% of FCS in the presence of 2 mg/mL of a polyclonal anti-MPO rabbit antibody conjugated with the AlexaFluor-488 dye (AlexaFluor-488, labeling kit for rabbit IgG). The use of a conjugated MPO mAb in our experiments allowed detecting MPO in mDC without permeabilization, thus ensuring that the signal only derived from material taken up from NET threads.

Induction of neutrophil apoptosis and necrosis

Neutrophils freshly isolated from the spleen were rendered apoptotic by incubating them with Fas/CD95 (from BD Biosciences) agonistic mAb. Less than 5% of cells were necrotic as assessed by trypan blue dye exclusion and 7-amino-actinomycin D (7-AAD) incorporation. Nevertheless, preparations were washed to remove necrotic debris before use. Necrosis was induced in naive PMNs with 4 cycles of freezing (liquid nitrogen) and thawing (37°C), leading to complete fragmentation of the cells, with $< 1\%$ intact cells remaining. To confirm apoptosis and necrosis, cells were stained with FITC-anti–mouse GR-1 and PercPcy5.5 anti–mouse CD11b, allophycocyanin-conjugated annexin V, and 7-AAD (all from e-Bioscience) according to the manufacturer's instruction.

DC-PMN coculture for immunization experiments

PMNs were seeded onto poly-D-lysine–coated tissue culture dishes in IMDM 2% FCS, allowed to adhere for 30 minutes, and added to mDCs (1:1; PMNs/DCs) for 16 hours. DCs were then recovered from the coculture through immune-magnetic separation after washing cultured cells with EDTA 0.2mM. mDCs were then identified and quantified by hemocytometry based on the typical hairy appearance and injected intraperitoneally (2.5×10^6 cells, once a week for a total of 6 injection) into naive mice.

We performed a total of 3 experiments for each type of immunization (mDCs alone, PMNs alone, DCs + PMNs, DCs + PMNs + DNAse) with 5 mice/group. The sera from immunized mice were evaluated for the presence of autoantibodies starting 1 month after the last immunization, for 3 consecutive months. Kidneys and lungs were evaluated for damage 3 months after the last immunization. Experiments requiring NET inhibition by DNAse were performed by adding DNAse (100 U/mL) to PMNs along the coculture with mDCs.

ELISA measurement of serum autoantibodies

To detect autoantibodies in the serum of immunized mice, we used different ELISA kits. Quantitative determination of MPO-ANCA (IgG) and PR3-ANCA (IgG) were performed with kits from Cusabio (CSB-E08676m) and USCN (E91434Mu), respectively. Determination of dsDNA, ssDNA, and ANA Ab was performed with kits from Alpha Diagnostic (#5110, 5210, and 5310).

Histopathology and immunohistochemistry

The severity of the renal damage in immunized and control mice was assessed by histopathologic analysis. A total of 9 mice (3 randomly chosen from each immunization experiment) have been analyzed and scored. A modified version of the National Institutes of Health semiquantitative scoring system for human lupus nephritis was adopted.[18] The following variables relative to glomerular and tubulointerstitial lesions were analyzed: glomerular cellularity, glomerular necrosis, glomerular crescents, glomerular sclerosis, interstitial inflammatory infiltration, and interstitial fibrosis. Glomerular and tubulointerstitial morphologic lesions were graded on a semiquantitative scale ranging from 0 to 3: 0 = absence of lesions; 1 = lesions involving up to 25% of the component considered; 2 = lesions

involving 25%-50%; and 3 = lesions involving > 50% of the component. The overall renal parenchyma damage score was determined by summing the scores relative to each of the variables. The histopathologic score was independently evaluated by 2 of the authors with specific training in mouse pathology (C.T. and S.S.). Cases in which the individual scores were discordant were discussed under a 2-headed microscope until consensus was reached.

Vasculitic pulmonary lesions were analyzed and scored according to a semiquantitative scoring system based on the histomorphologic analysis of vascular areas. Briefly, the extension and intensity of the inflammatory infiltrates involving lung vessels were graded as follows: extension-0 = absent; extension-1 = focal lesion; extension-2 = multifocal lesions; extension-3 = diffuse lesions; intensity-0 = absence of inflammatory cell infiltration; intensity-1 = perivascular infiltration partially encircling vessels; intensity-2 = perivascular infiltration totally encircling vessels with extension to the vessel wall; and intensity-3 = inflammatory infiltration effacing vessel wall architecture.

For immunohistochemistry, sections (8 μm) were incubated with anti–mouse Ly6G (GR-1, BD Biosciences), anti–mouse C3 (Abcam), and polyclonal goat anti–mouse AlexaFluor-488 for the analysis of neutrophilic infiltration of C3 or IgG deposition, respectively.

In situ detection of PMN-DC interaction

PFA-fixed skin biopsies from 6 patients diagnosed with microscopic polyangiitis, 5 patients diagnosed with SLE, and 5 patients diagnosed with psoriasis (supplemental Table 1, available on the *Blood* Web site; see the Supplemental Materials link at the top of the online article), were selected for in situ analysis of NETotic PMN-DC interaction. Four-micrometer-thick sections were cut and mounted onto slides. Sections underwent either double-immunohistochemistry or double-immunofluorescence staining for the PMN marker MPO and for the mDC marker DC-Sign (CD209). Double immunostainings were performed as previously reported.[19] Briefly, sections underwent antigen retrieval with pH 6 citrate buffer and were subsequently treated with blocking buffer (Novocastra). Two consecutive rounds of immunostaining were then performed using unconjugated primary antibodies against MPO (mouse-anti–human monoclonal antibody, clone 59A5, Novocastra) and DC-Sign (rabbit anti–human polyclonal antibody, Abcam). For immunohistochemistry, binding of primary antibodies was detected by species-specific secondary antibodies and revealed by the peroxidase ($LSAB^+$ kit HRP, Dako Denmark) or alkaline phosphatase ($LSAB^+$ kit AP, Dako Denmark) method. Immunostained sections were then counterstained with hematoxylin and evaluated under a Leica DM 2000 optical microscope using 20× (numeric aperture 0.4) and 40× (numeric aperture 0.65) objective lenses. Microphotographs were collected using a Leica DFC 320 digital camera and the Leica IM50 imaging software (Leica Microsystems). Double immunofluorescence was performed using secondary antibodies conjugated with Alexa-488 and Alexa-546 fluorochromes and the nuclear dye Draq5. Sections were analyzed with the confocal microscope Microradiance 2000 (Bio-Rad Laboratories) equipped with Ar (488 nm), HeNe (543 nm) and Red Laser Diode (638 nm) lasers. Confocal images (512 × 512 pixels) were obtained using a 20×, 0.5 NA Plan Fluor DIC or 60×, 1.4 NA oil immersion lens and analyzed using ImagePro 7.0.1 software. Immersion oil (ISO 8036) was from Merck.

Statistical analysis

Continuous and categorical variables were compared using the Mann-Whitney *U* test, using Prism Version 5.0d software (GraphPad).

Correlation between variables was assessed using Pearson and Spearman correlation coefficients using the Statistical Package for the Social Sciences Version 13.0 (IBM) software. Analysis of the effects of different types of immunization on generation of autoantibodies was performed by 1-way ANOVA with posttest Dunn correction, using Prism Version 5.0d software (GraphPad).

Results

Inflammatory skin-elicited PMNs are prone to NETosis

We used our previously described agar trap method to collect elicited neutrophils from subcutaneous implants.[15] With this method, leukocytes could be easily recovered over 5 days, and PMN enriched up to 95% (supplemental Figure 1). These PMNs are activated, produce reactive oxygen species (ROS), and die within 24 hours by apoptosis, and NETosis (Figure 1A), NETosis could be detected by seeding PMNs onto poly-lysine–coated glasses for the visualization of extruded DNA threads decorated with the antimicrobial proteins MPO, PR3, and elastase (supplemental Figure 2). To quantify NETosis and to distinguish NETosis from apoptosis, the cell-impermeable DNA dye SYTOX green was added to PMNs such to measure the size of released nuclear contents from micrographs, using the software-assisted technique described by Metzler et al[20] (supplemental Figure 3). Figure 1B and C shows that agar-PMNs spontaneously and even more efficiently formed NETs than PMA treated PMNs isolated from the spleen[5] (Figure 1A). Spontaneous NET formation from ex vivo–isolated PMNs physiologically depends on the inflammatory microenvironment in which granulocytes are generated. Indeed, granulocytes obtained from agar plugs subcutaneously implanted into TNF-KO and IFNγ-KO mice were unable of NETosis (supplemental Figure 4) in line with in vitro data showing that TNF can directly activate neutrophils[21] and that IFNs act as priming factors on mature neutrophils for NET formation.[22] Notably, both IFNγ-KO and TNF-KO mice did not show defective PMN recruitment. On the contrary, the absence of IL-6, which was associated with an increased PMN recruitment (not shown), did not impair NET formation (supplemental Figure 4). Thus, we showed that the agar-trap method is adequate for the ex vivo collection of NETosis-prone PMN (from here and thereafter referred as NETotic PMN).

BM-derived mDC uptake PMN components after interaction with NET

The breakdown of tolerance to neutrophil components, such as MPO and PR-3, occurring during ANCA-associated systemic vasculitis,[23] requires the transfer of neutrophil-derived antigens to professional antigen-presenting cells, their activation, and antigen cross-presentation to T and B cells. To evaluate whether NETotic PMNs were able to interact with mDCs, live cell imaging experiments were performed coculturing mDCs, stained with the vital dye PKH-26, with inflammatory PMNs prone to NETosis, in which the dsDNA of NETs was stained with the SYTOX green dye. During the coculture, NETotic PMNs were found to stably interact with mDCs, whereas intact PMNs and PMNs dying of apoptosis only tethered mDCs transiently (Figure 2A; supplemental Movie 1). Notably, on overnight coculture, such interaction resulted in mDC uploading with NET components, including DNA (not shown), and neutrophil proteins, such as PR3 and MPO (Figure 2B). To evaluate the different efficacy of antigen uploading into mDCs by NETotic and apoptotic PMNs, mDCs were also cocultured with apoptotic PMNs obtained by incubating naive PMNs in the presence of a Fas-triggering Ab. Although not present in our PMN culture, necrotic PMNs, obtained by freeze and thaw, were used as further control because described by others as potential vehicle of neutrophil autoantigens.[24] Confocal microscopy and software-assisted micrograph quantification and analysis showed efficient uploading of both PR3 and MPO from agar-elicited

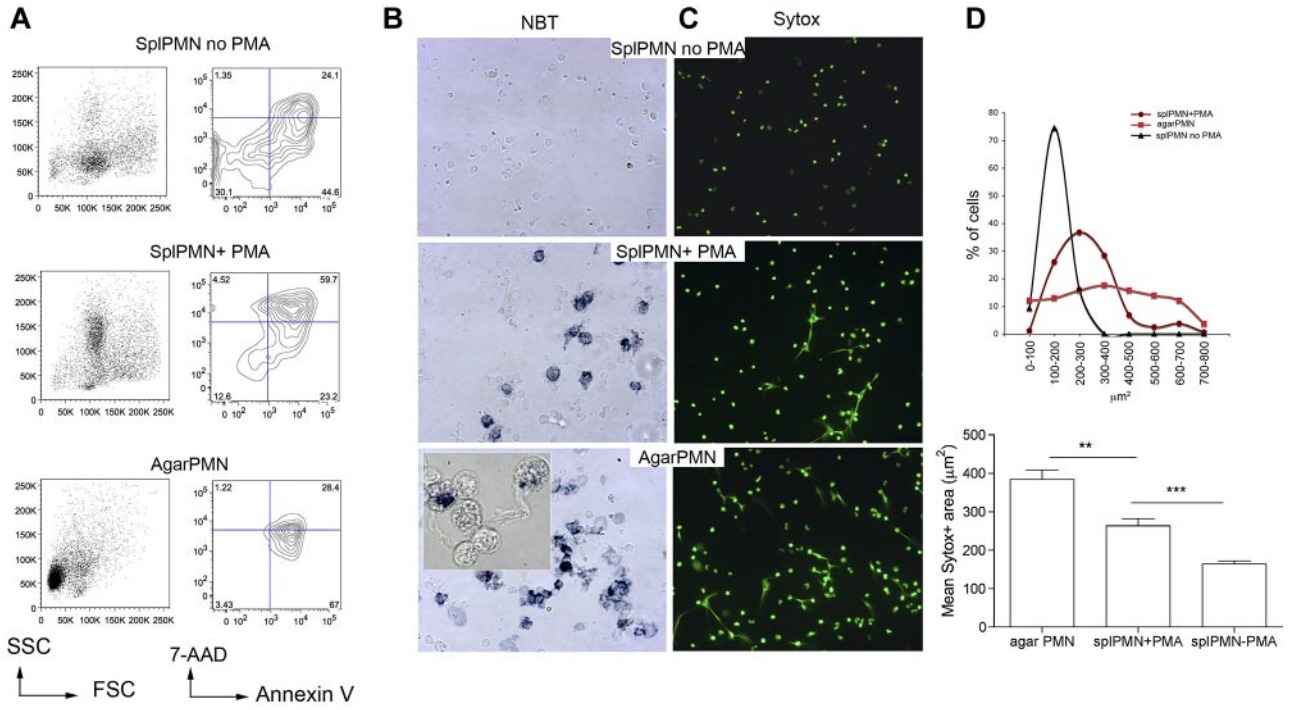

Figure 1. Inflammatory, agar-elicited neutrophils spontaneously die of NETosis ex vivo. (A) PMN cell death was evaluated by annexin V/7-AAD staining of CD11b$^+$Gr-1$^+$ cells. Early apoptotic cells (annexin V$^+$/7-AAD$^-$), apoptotic cells (annexin V$^+$/7-AAD$^+$), necrotic cells (annexin V$^-$/7-AAD$^+$), and live cells (annexin V$^-$/7-AAD$^-$) were identified. Representative forward scatter (FSC) and side scatter (SSC) plots are shown. (B) Activation of NADPH oxidase in PMNs from agar and in PMA-treated naive PMNs seeded onto poly-D-lysine–coated glasses. Activation of NADPH oxidase was qualitatively evaluated using the nitroblue tetrazolium (NBT) reduction test. Contrast-phase pictures obtained under a light microscope show that both agar-PMNs and naive PMNs treated with PMA produce ROS (blue precipitate). (C) Representative IF analysis shows a more efficient NETosis in agar-collected than PMA-treated spleen-derived PMNs (original magnification ×20). SYTOX green DNA dye was added to PMN after their fixation with 4% PFA. (D) Quantification of NET formation in agar-collected and PMA-treated neutrophils. Nuclear area of agar-PMN and PMA-treated neutrophils is plotted against the percentage of SYTOX-positive cells corresponding to a given nuclear area. PMNs undergoing NETosis have a broad range of nuclear areas, whereas apoptotic neutrophils show smaller nuclear areas, less distributed and composed within a narrow peak (top panel). In line, agar-PMNs showed higher mean nuclear area compared with PMA-treated spleen PMN (bottom panel). In this experiment, the SYTOX green DNA dye was added to PMNs after PFA fixation 18 hours later. Experiments comparing agar-PMNs with PMA-treated PMNs were repeated 6 times with PMNs from at least 3 donor mice each. Number of nuclei analyzed/experiment = 200.

NETotic PMNs, which were detectable as dotted green fluorescence (Figure 2C). The interaction between DCs and apoptotic PMNs allowed the uptake of both PR3 and MPO by mDCs, but the transfer of these antigens was less conspicuous than that occurring in the presence of NETotic PMNs, as visualized by staining the coculture with specific Alexa-488–conjugated anti-PR3 and MPO antibodies (Figure 2C-E). Moreover, PMN cytoplasmic antigens derived from apoptotic PMNs showed predominant localization within large apoptotic bodies (Figure 2F).[25] By contrast, necrotic PMNs failed to transfer detectable amounts of PR3 and MPOs to mDCs (Figure 2C-E). Therefore, the formation of NET threads represents the most effective form of PMN cell death for the transfer of cytoplasmic antigens to mDCs toward potential antigen processing and presentation. To further confirm this finding, mDC/NETotic-PMN interaction was tested in the presence of DNAse, which selectively digests NET DNA threads (Figure 3A-B) without affecting PMN activation and ROS production (supplemental Figure 5)[26] and leaving intact the vast majority of apoptotic cells and PR3-containing apoptotic bodies (Figure 3B arrows; and annexin V$^+$ cells in Figure 3C).[25] We found that DNAse prevented PR3 and MPO uploading into mDCs (Figure 3D-F), indicating that NET integrity is required for efficient transfer of PMN autoantigens to mDCs.

These experiments highlight a relevant difference among NETotic, apoptotic, and necrotic PMNs in the capacity of transferring neutrophil autoantigens to mDCs. Such a difference, probably relevant for the development of autoimmunity, would not be appreciated by the sole analysis of phenotypic changes associated with mDC maturation/activation because comparable up-regulation of mDC activation markers (eg, CD40) and similar mDC migration to mesenteric lymph nodes on intraperitoneal injection in vivo (supplemental Figure 5) occurred regardless the type of PMN death.

Immunization with NET-loaded DCs induces ANCA and autoimmune vasculitis in mice

The experiment providing clear-cut information on which type of PMN death is relevant for ANCA induction is the immunization of naive mice with mDCs cocultured with apoptotic, necrotic, or NETotic PMNs in the presence or in the absence of DNAse. The use of DNAse allowed discerning the contribution of NET, whose DNA threads carrying cytoplasmic antigens is disrupted by DNAse activity (Figure 3A-B), from that of apoptotic PMNs (Figure 3B arrows, and annexin V$^+$ in Figure 3C), which are not affected by DNAse. Thus, mice were repeatedly (6 times) immunized by intraperitoneal injection of mDCs that underwent coculture with NETotic PMN, also in the presence of DNAse, or that have been cultured with apoptotic or necrotic neutrophils. As further controls, mice were immunized with unloaded mDCs or NETotic PMNs, separately. Three months after the last immunization, mice were evaluated for development of autoantibodies in the serum and for signs of autoimmune vasculitis in the kidney and lung parenchyma.

We found that mice immunized with mDCs loaded with NET content showed a significant induction of ANCA and anti-dsDNA

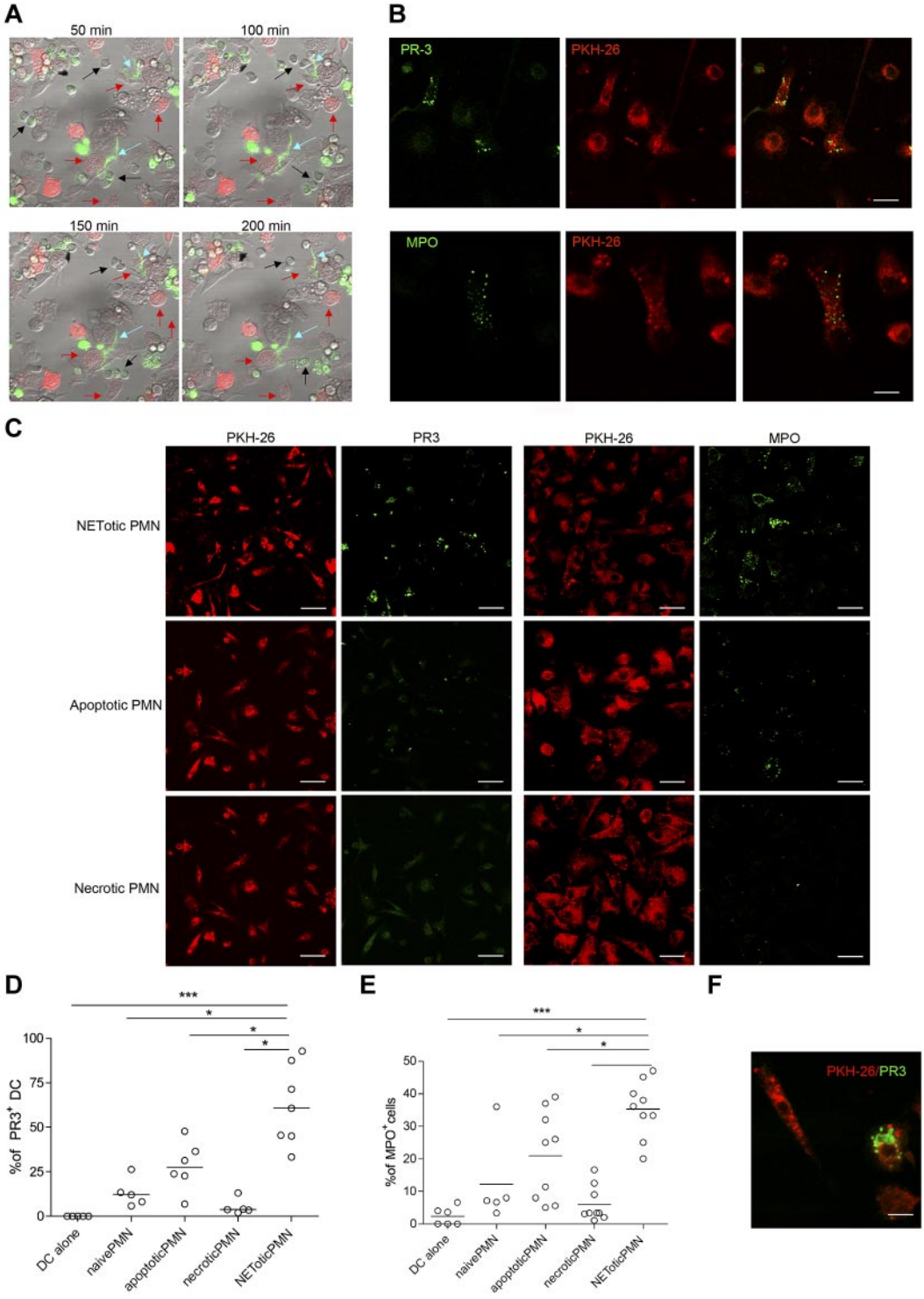

Figure 2. mDCs interact with NETotic PMNs and are loaded with proteins from NET. (A) NETs persistently interact with mDCs. In this live imaging experiment, agar-PMNs were seeded onto culture dishes and allowed to adhere 30 minutes before adding mDCs previously labeled with the membrane vital dye PKH-26. The cocultures were also performed in the presence of the DNA dye SYTOX green, which stains only PMNs undergoing NETosis. The coculture was maintained o/n in a humidified chamber under confocal microscope, acquiring a picture every 10 minutes to highlight any interaction between PMNs and mDCs. PMNs in the cellular mixture form NETs (turquoise arrows) and NETs interact with mDCs (red arrows). Black arrows indicate naive neutrophils. Scale bars represent 5 μm. (B) Uploading of mDCs with NET components. After NET interaction, mDCs are uploaded with the neutrophil protein PR3 and MPO. In this live imaging experiment, labeled PKH-26 mDCs were added to agar-PMN in the presence of a mAb to PR3 or MPO directly conjugated with Alexa-488 dye. After 18 hours, cells were fixed with PFA 4% and observed under a confocal microscope. Scale bars represent 10 μm. One representative experiment of 5 performed. (C) Uploading of PR3 and MPO by mDCs tested in the presence of different type of PMN death. Apoptotic PMNs, generated by Fas triggering Ab and necrotic PMNs obtained by freeze and thaw, were compared with NETotic PMNs for their capability to transfer PR3 and MPO to mDCs in coculture experiments. Representative confocal IF analysis showing that necrotic PMNs almost failed to transfer neutrophil PR3 or MPO to mDCs; on the contrary, PR3 and MPO were detectable as dotted green fluorescence in mDCs that interacted with NETotic PMNs and, to a lesser extent, in mDCs cultured with apoptotic PMNs. (D-E) Software-assisted micrograph quantification of mDCs uploading of PR3 (D) and MPO (E) performed on a total of 200 cells that were imaged by confocal microscopy. DCs cultured with naive PMNs, maintained alive by incubating them in the presence of 30% of FCS and DCs alone. were the negative controls for PR3 transfer and MPO. Scale bars represent 30 μm. (F) Appearance of $PR3^+$ apoptotic bodies that are taken up by mDCs cocultured with apoptotic cells.

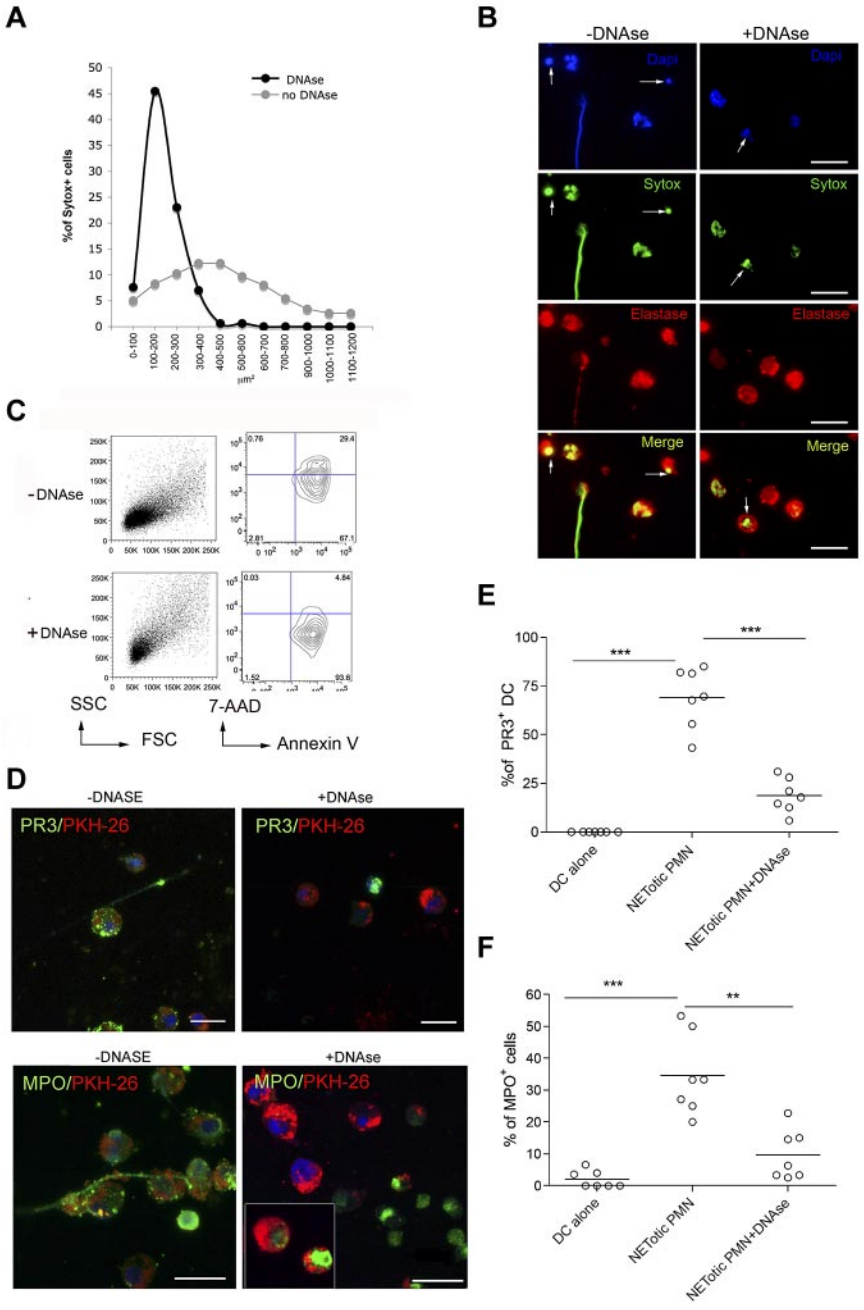

Figure 3. DNAse treatment of mDC-PMN coculture abrogates DC uploading with neutrophil proteins. (A) Quantification of NET formation by agar-elicited neutrophils seeded onto poly-D-lysine–coated glasses in the presence of DNAse. Nuclear areas of PMNs are plotted against the percentage of SYTOX-positive cells corresponding to a given nuclear area. In the presence of DNAse, nuclear areas appear smaller and show a narrow peak compared with untreated PMNs in which nuclear area has a broad distribution. Number of nuclei analyzed/experiment = 200. One representative experiment of 3 performed. (B) IF analysis of agar-PMN seeded onto poly-D-lysine-coated glasses in the presence of DNAse (100 U/mL) and DNA dye SYTOX green. Twenty-four hours later, PMNs were fixed and stained with a polyclonal Ab to elastase. Scale bars represent 10 μm. One representative experiment of 3 performed is shown. (C) Forward scatter (FSC)/side scatter (SSC) and annexin V/7-AAD representative plots for $CD11b^+GR\text{-}1^+$ agar-PMNs treated or not with DNAse, showing the presence of annexin V^+ apoptotic cells in agar-PMNs that have been cultured onto poly-D-lysine–coated glasses also in the presence of DNAse. (D-F) Incorporation of PR3 and MPO in mDCs was prevented by DNAse treatment. (D) Confocal microscopy analysis of mDCs ($PKH\text{-}26^+$, red) cocultured o/n with NETotic PMN in absence (left panels) or presence (right panels) of DNAse and Abs to PR3 or MPO conjugated with Alexa-488 dye. The vital DNA dye Draq 5 (blue) shows that only the DNA of PMNs but not of DCs is degraded by DNAse. Notably, PMNs treated with DNAse retain both PR3 and MPO staining. Scale bars represent 10 μm. One representative experiment of 5 performed. Quantification of PR3 (E) and MPO (F) incorporation by mDCs performed on confocal microscopy micrographs using the software-assisted technique. Number of cells analyzed = 200. One representative experiment of 3 performed.

autoantibodies in the serum compared with those immunized with mDCs or NETotic PMNs alone (Figure 4). Mice immunized with DCs loaded with apoptotic PMNs displayed a similar pattern of autoantibodies to that of mice immunized with mDCs loaded with NET content (Figure 4). In these mice, however, a less conspicuous development of MPO-ANCA was observed along with a higher titer of anti–ss-DNA Abs (Figure 4C). Grippingly, the induction of ANCA was associated with the development of an autoimmune vasculitis detectable in the renal (Figure 5) and pulmonary parenchyma (supplemental Figure 6) of the mice immunized with mDCs loaded with NET content. In these mice, the autoimmune damage in the renal parenchyma ranged from moderate to severe (Figure 5A) and was characterized by signs of extracapillary glomerulonephritis and/or tubulointerstitial nephritis with vascular neutrophilic infiltration (Figure 5; supplemental Figure 7) and complement and IgG deposition (supplemental Figure 8). The renal damage observed in mice immunized with NET-loaded mDCs is evocative of an autoimmune SVV characterized by a pleomorphic inflammatory infiltration dominated by neutrophil accumulation, whose intensity correlates with the amount of serum MPO-ANCA (supplemental Figure 9). In addition, a minority of mice also developed alopecia (supplemental Table 1). The autoimmune features observed in immunized mice, which are summarized in supplemental Table 1, are shared by human autoimmune systemic vasculitides, including ANCA-related paucimmune vasculitides and lupus vasculitis, in line with the development of overlapping autoantibody patterns in these systemic autoimmune diseases. Consistent with the in vitro results of the coculture experiments, the autoimmune phenotype observed in mice immunized with mDCs cocultured with NETotic PMNs, including the induction of ANCA

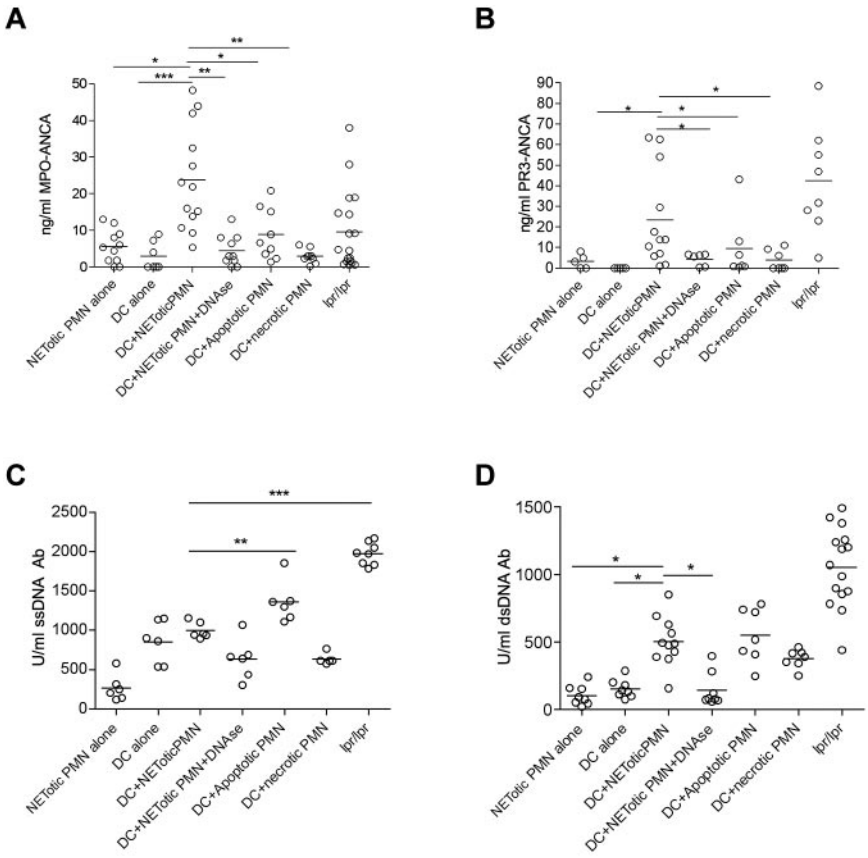

Figure 4. In vivo injection of NET-loaded mDCs induces autoantibody production. Level of anti–MPO-ANCA (A), PR3-ANCA (B), ss-DNA (C), and ds-DNA (D) Ab in mice immunized with DCs loaded with NET contents in the presence or absence of DNAse, as well as in mice immunized with mDCs cocultured with apoptotic or necrotic PMNs. The induction of MPO and PR3-ANCA as well as of anti–ds-DNA autoantibodies in mice immunized with NET-loaded DCs was significantly reduced by the use of DNAse in the coculture. Immunization of mice with DCs cocultured with apoptotic PMNs induced PR3 and MPO-ANCA development but less efficiently than DCs loaded with NETotic PMNs. On the contrary, DC/apoptotic PMN immunization generated the highest titer of anti–ss-DNA Ab. Other controls were obtained by immunizing mice with DCs or PMNs alone. Each dot represents a single mouse. Median values are given. *$P < .05$ (1-way ANOVA with posttest Dunn correction). **$P < .01$ (1-way ANOVA with posttest Dunn correction). ***$P < .001$. *Fas* mutant *lpr-lpr* mice were used as positive control for autoantibodies.

autoantibodies, was impaired by DNAse treatment (Figures 4 and 5; supplemental Figure 6), further supporting that the NET structural integrity is required for the transfer of NET antigens to mDCs and the induction of autoimmunity. Interestingly, mice immunized with mDCs cocultured with apoptotic PMNs, despite the development of detectable levels of ANCA, did not develop kidney or lung vasculitis (Figure 5; supplemental Figure 6). In line, Patry et al have shown that rat immunization with syngenic apoptotic neutrophils induced ANCA but not vasculitis.[27] Although the immunization protocol adopted by Patry et al differs from our own, the outcome is rather concordant, indicating that the antigen transfer from apoptotic PMNs to DCs is not sufficient to induce vasculitis despite the ability of breaching the tolerance to some cytoplasmic neutrophil antigen.

Correlation between ANCA, vasculitis, and spontaneous NETosis in lpr/lpr mice

In SLE, the chronic inflammatory and autoimmune condition is associated with the presence of a varied pattern of autoantibodies that are, for the majority, directed against nuclear components. A minority of SLE patients has been reported to develop ANCA (mainly MPO-ANCAs) but, differently from SVV, the pathogenic role of these autoantibodies in SLE is not clear. Contrasting works have reported the presence[28] or the absence[29,30] of correlation between serum ANCA levels and disease activity in SLE. In a large cohort of SLE patients, serum ANCA levels were found to be correlated with specific clinical manifestations, such as serositis, livedo reticularis, and arthritis.[31] Nevertheless, the direct role of ANCA in the vascular damage that may occur in SLE patients,[32] although postulated,[33] still remains debated. According to our hypothesis of NET triggering ANCA and autoimmune vasculitis, a direct correlation among NETosis, ANCA, and vasculitic lesions, but not among NETosis, ss-DNA/ds-DNA Abs, and nephritic lesions, could be envisaged in the SLE pathologic setting. To verify this hypothesis, *lpr/lpr* mice, which spontaneously develop a SLE-like disease, were analyzed for the development of ANCAs. We found that, similarly to the human condition, 30% of these mice developed ANCAs, whereas almost all mice developed comparable levels of ss-DNA/ds-DNA Abs (Figure 6). To correlate the development of ANCA with NETosis, 8 *lpr/lpr* mice with variable ANCA but similar ss-DNA/ds-DNA Abs levels were analyzed for spontaneous NETosis of spleen-purified PMN as described in Figure 1. PMNs from *lpr/lpr* mice showed a distribution of $SYTOX^+$ nuclear area that varied from low values indicative of apoptosis to high values, suggestive of NETosis (Figure 6). To test the association between NETosis and ANCAs or ss-DNA/ds-DNA Abs levels, the total $SYTOX^+$ area calculated > 200 cells for each mouse, was correlated with the amount of individual mouse antibodies through a linear regression analysis. NETosis positively correlated with MPO-ANCA ($r^2 = .9048$, $P = .046$) and PR3-ANCA ($r^2 = .7857$, $P = .0279$) but not with ss-DNA/ds-DNA Abs. We subsequently analyzed the renal and pulmonary parenchyma of the same *lpr/lpr* mice, to further correlate ANCA and NETosis with the development of autoimmune vasculitis. Although these mice showed similar overall histopathologic score of renal damage, only mice with the highest ANCA levels displayed more intense renal tubulointerstitial lesions, particularly vasculitic lesions. Cases in which the pattern of autoantibodies was dominated by ss-DNA/ds-DNA Abs rather than ANCA prevalently showed glomerular nephritic lesions (Figure 6).

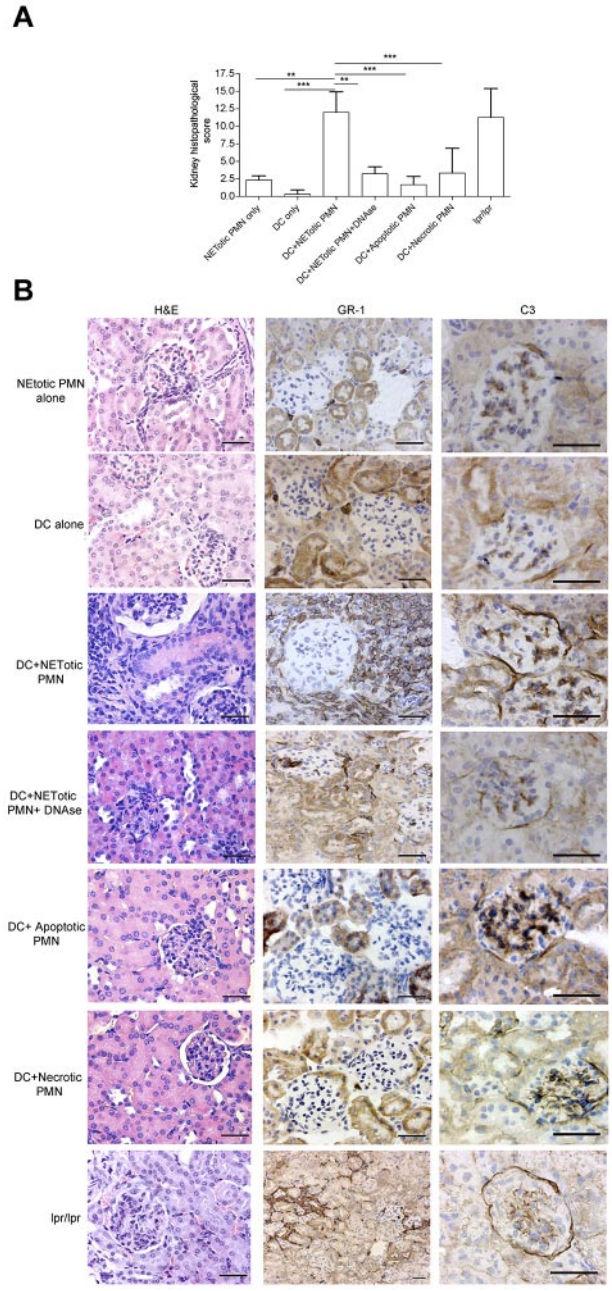

Figure 5. NET-loaded mDCs injected in mice induce renal damage. (A) Histopathologic grading of renal damage in mice immunized with mDCs loaded with NET contents, in the presence or absence of DNAse, as well as in mice immunized with mDCs loaded with apoptotic or necrotic PMNs, mDCs, or PMNs alone (n = 9/group). $^{**}P < .01$ (1-way ANOVA with posttest Dunn correction). $^{***}P < .001$. Data are mean ± SD. (B) Histopathology showing renal damage in mice immunized as in panel A. Figure shows hematoxylin and eosin staining and IHC for neutrophil infiltration (GR-1 Ab), and C3 deposition. Only kidneys from mice immunized with DCs loaded with NET components showed extended parenchymal damage with vascular and periglomerular neutrophilic infiltration and complement deposition. This phenotype was prevented in mice immunized with mDCs cocultured with NETs in the presence of DNAse. One representative mouse/group. Scale bars represent 50 μm. Representative autoimmune *fas* mutant *lpr-lpr* mice used as positive control for renal damage showing the typical glomerular and interstitial nephritis.

We then reasoned that, if NETs were the true source of autoantigens triggering ANCAs, the sera from mice in which vasculitis has been induced should recognize NET in vitro. Consistently, sera from mice immunized with mDC + NETotic PMN or from *lpr/lpr* mice and characterized by ANCA and vasculitic lesions, stained NET induced in vitro by PMA. DNAse treatment of PMA-exposed PMN abolished the specific recognition of NET structures but not the staining of non-NETotic PMNs and debris observed in the presence of high ss-DNA/ds-DNA Ab titers characterizing most *lpr/lpr* immune sera (supplemental Figure 10).

Thus, ANCA recognized PMN antigens made available through NETosis. This suggested that not only the immunogenicity of PMN-associated proteins but also their recognition by ANCA was strictly dependent on their conformational status associated with NET formation.

Considering that Ab from *lpr/lpr* mice are polyreactive and capable to recognize human proteins, we tested whether sera from mice immunized with DC + NETotic PMNs also stained human peripheral blood leukocytes. We found that sera from both DC + NETotic PMNs immunized and *lpr/lpr* mice reacted with human PMNs, although with a different pattern. Sera from DC + NETotic PMNs immunized mice showed a diffuse cytoplasmic staining according to their enrichment in ANCAs, whereas sera from *lpr/lpr* mice showed a nuclear and perinuclear pattern according to the prevalence of ss-DNA/ds-DNA Abs over ANCAs (supplemental Figure 10).

DC interaction with NETotic PMNs can be visualized in human autoimmune disease

We next evaluated whether the above-demonstrated pathogenic role of NET in inducing ANCA through the interaction with mDCs could find a potential correlative picture in human pathology. To this end, we evaluated skin lesions from 6 patients diagnosed with MPO-ANCA–associated microscopic poliangiitis (MPA), 5 patients with SLE, and 5 patients with psoriasis, for the presence of mDCs interacting with MPO^+ PMNs (supplemental Table 2). In MPA samples, mDCs intermingling with MPO^+ neutrophils were detected along with scattered mDCs showing cytoplasmic reactivity for MPO, which suggested their uploading of neutrophil antigens (Figure 7A). Moreover, within the vascular inflammatory infiltrates of these cases, which were rich in MPO^+ neutrophils, we detected extracellular MPO suggestive of NET in close contact with $DC\text{-}SIGN^+$ cells (Figure 7B black arrows). A similar picture of NET structures in close contact with $DC\text{-}SIGN^+$ mDCs was observed in samples from SLE patients, which also clearly showed mDCs loaded with PMN apoptotic bodies (Figure 7B green arrows). By contrast, in skin samples from psoriatic patients, the formation of NET structures was inconspicuous and the direct interaction between PMN and mDCs was not observed (Figure 7B). The in situ spatial interaction between NETs and mDCs was also visualized by double immunofluorescence on confocal microscopy using MPO and DC-SIGN (Figure 7C arrows) in MPA samples. Overall, these data strongly suggest an interaction between NETs and mDCs in the pathologic setting of human SVV, which might underlie the above-demonstrated dynamics of ANCA induction in mice.

Discussion

Herein, we show, for the first time, that NETs are able to transfer PMN cytoplasmic antigens to DCs, which are in turn responsible for triggering adaptive immune responses characterized by pathogenic ANCA production.

Although neutrophils have been directly implicated in autoimmune tissue damage through the release of ROS, their actual role in ANCA development and associated autoimmunity was still unclear.

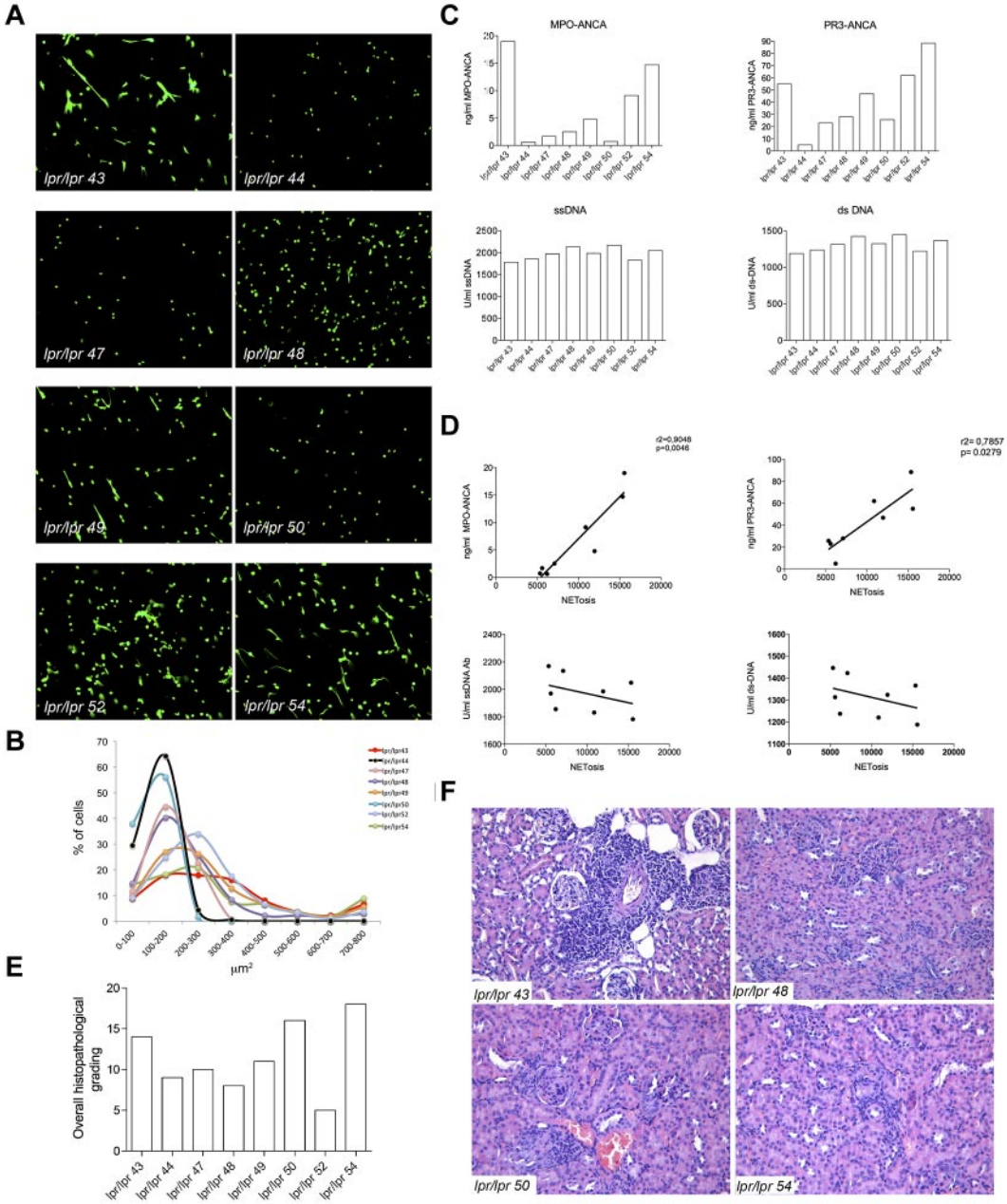

Figure 6. Correlation between NETosis, ANCAs, and autoimmune vasculitis in lupus-prone mice. (A) Spleen PMNs isolated from 8 *lpr/lpr* mutant mice were tested for spontaneous NETosis. PMNs were seeded onto polylysine-coated glasses without PMA or any type of stimuli, fixed and stained with the SYTOX green DNA dye. PMNs from every single mouse were imaged through confocal microscopy. Spleen purified PMNs normally die of apoptosis when cultured o/n in the absence of any stimuli (as shown in Figure 1), whereas PMNs from the same *lpr/lpr* mice showed enrichment in NETosis other than dying of apoptosis. Grippingly, PMNs from mice #44, 47, 48, and 50 only showed apoptosis, whereas PMNs from mice #43, 49, 52, and 54 clearly showed signs of NETosis. (B) Quantification of NET formation was performed by plotting SYTOX$^+$ nuclear areas against the percentage of SYTOX$^+$ cells corresponding to a given nuclear area. Number of nuclei analyzed/experiment = 200. (C) Level of MPO-ANCA, PR3-ANCA, ss-DNA, and ds-DNA Abs in the same *lpr/lpr* mutant mice analyzed in panel A. (D) Correlation between NETosis and MPO and PR3-ANCA. NETosis correlated with both MPO and PR3-ANCA ($r^2 = .9040$, $P = .046$; and $r^2 = .7857$, $P = .0279$, respectively) but not with the different types of ANA. (E) Histopathologic grading of the overall renal damage in the same *lpr/lpr* mutant mice described in panel A. (F) Hematoxylin and eosin staining shows intense renal tubulointerstitial lesions, particularly vasculitic lesions, in mice with higher ANCA titers (*lpr/lpr* 43 and 54), whereas in cases with lower ANCA titers, in which autoantibody patterns were dominated by ds- and ss-DNA ANA antibodies, glomerular nephritic lesions are prevalent (*lpr/lpr* 48 and 50).

Immune cells dying of apoptosis or necrosis are promptly eliminated by macrophages. An excess of cell death or defective macrophage scavenging allows uptaking of cell remnants by immature DCs for degradation, processing and presentation that in the presence of proper costimulatory signals allows T-cell activation.[34] Impaired clearance of apoptotic neutrophils has been implicated in several autoimmune diseases, such as SLE, in humans[35,36] and mice,[37] whereas its role in ANCA development is less established. The unsolved issue is the break of tolerance toward proteins that are normally retained within neutrophil cytoplasm. PR3 and MPO are the 2 major immunogenic proteins recognized by ANCA. This implies that these proteins should become available for antigenic recognition by immune cells. The reactivity of ANCA with the surface of unprimed apoptotic

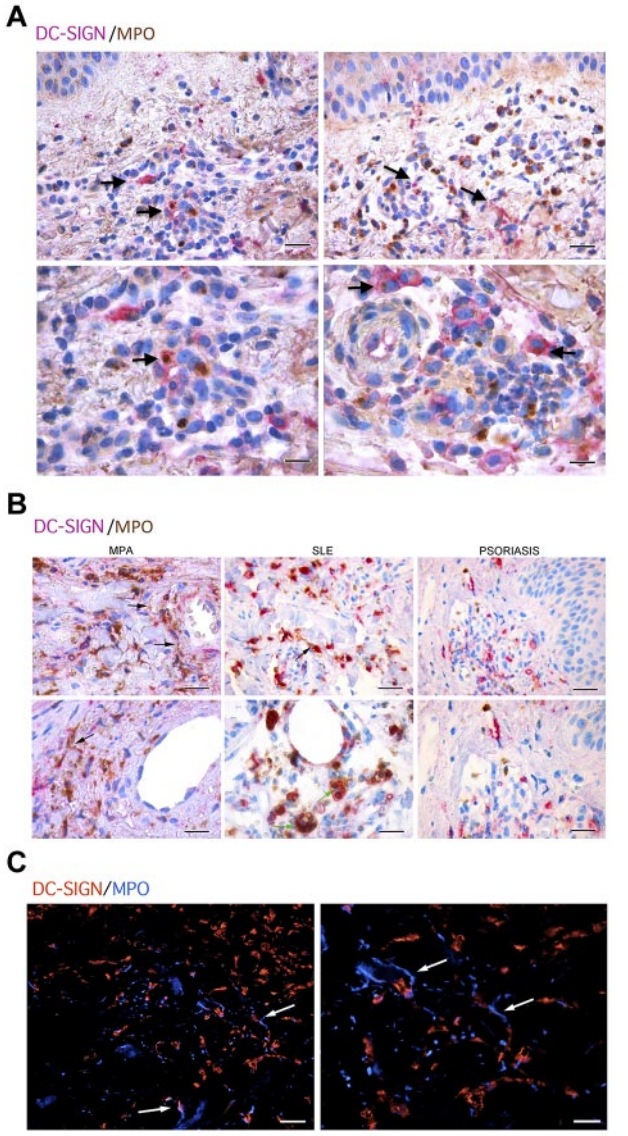

Figure 7. mDC-neutrophil interaction in skin biopsies from patients with MPO-ANCA–associated microscopic poliangiitis. (A) Double immunostaining with anti–DC-SIGN (purple) and anti-MPO (brown) shows mDCs intermingling with PMNs and populating the inflammatory infiltrate (top panels, black arrows; scale bars represent 25 μm). Higher magnifications highlight mDCs loaded with MPO (bottom panels, black arrows; scale bars represent 10 μm). (B) Within the inflammatory infiltrate involving dermal vessels of ANCA-associated MPA patients or in the skin of SLE patients, extracellularly located MPO, suggestive of NETs (black arrows), can be detected in close proximity with DC-SIGN$^+$ cells (left panel, scale bar represents 25 μm; right panel, scale bar represents 10 μm). SLE skin biopsies also showed mDCs loaded with PMN apoptotic bodies (green arrows). On the other hand, in skin biopsies from psoriasis, DC-SIGN$^+$ cells are not in contact with the few MPO$^+$ cells that are present. (C) In situ immunofluorescence microscopy on the same samples highlighted the presence of NET (white arrows) in damaged areas as detected by DAPI nuclear staining (blue) and MPO (red; top panels). One representative biopsy from 1 of the 6 MPA patients analyzed is shown (original magnification ×40).

neutrophils and the translocation of PMN cytoplasmic granules to the cell surface of apoptotic PMNs[25,38] have suggested the idea that apoptotic cells might represent an effective source of neutrophil autoantigens. Accordingly, rat immunized with apoptotic neutrophils showed ANCA but unexpectedly failed to develop autoimmune vasculitis.[27] In line, we observed ANCA induction without vasculitis in mice immunized with mDCs loaded with apoptotic PMNs. In this light, it could be hypothesized that apoptotic PMNs may promote the development of nonpathogenic ANCA. In addition, in SVV, the prototypical ANCA-related autoimmune disease, elevated levels of granulopoiesis-related transcription factors (eg, CEBP-β) and cytokines (eg, G-CSF) have been recently implicated in the decreased rate of PMN apoptosis, which suggests a role for the types of PMN death other than apoptosis in the pathogenesis of ANCA-associated autoimmunity.[39] Would the factors involved in the enhanced granulopoiesis of SVV patients also be responsible for skewing PMN death from apoptosis to NETosis, the arousal of pathogenic ANCA may find an explanation. Here we show that NETosis, is both immunogenic and pro-inflammatory whereas apoptosis is known to be poorly effective in inducing inflammation.[40] Accordingly, impaired NET formation occurs in TNF- and IFNγ-KO mice, suggesting that inflammation is an effective inducer of NETosis also in the absence of pathogen infections. In addition, primary and secondary necrosis, differently from apoptosis, are endowed with more significant immunogenicity because of the release of DAMPs and danger signals, such as HMGB-1[41] promoting DC maturation. On this line, TLRs have been consistently involved in the pathogenesis of SLE and SVV.[42-44] However, in necrotic PMNs, proteins undergo structural changes that altering epitope conformation render MPO and PR3 unsuitable for DC cross-presentation of relevant epitopes. In NETtosis, the cytoplasmic proteins are extruded in association with a nucleic acid thread that preserves their conformation to grants their antimicrobial activity.

Thus, NET immunogenicity stems from the integrity of the DNA backbone that encloses and preserves the conformation of relevant antigens. Consistently, DNA digestion left untouched apoptotic/necrotic cells, whereas destroyed NET threads such to prevent mDC uploading of conformational preserved neutrophil antigens in vitro and consequently ANCA production and autoimmunity in vivo. This finding is relevant considering that most autoantibodies to neutrophil proteins PR3 and MPO recognize conformational epitopes.[13,14] Indeed, PR3-ANCAs from Wegener granulomatosis patients bind epitopes within the active site of PR3 and interfere with its enzymatic activity.[45] Similarly, MPO-ANCA can interfere with the interaction between MPO and its inhibitor ceruloplasmin, a notion supporting the conformation-dependent binding of epitopes for such autoantibodies. In agreement with our results demonstrating the necessity to preserve the integrity of NET DNA to promote mDC activation and loading, Lande et al recently showed that the NET-associated antimicrobial peptide LL37 protects DNA from extracellular degradation allowing NET DNA-mediated activation of pDCs.[9] The immune system is normally protected from the exposure and recognition of self-DNA. Excess release of nucleic acids or mutation in the *DNAse* gene could result in escape from protection.[46] Indeed, mutation in the *DNAse* gene was found associated with autoimmune disease as in humans SLE.[47]

In SLE, neutrophils are highly prone to form NET on binding to anti-RNP autoantibodies, a hallmark of this disease.[10] It has been recently shown that pDCs are able to respond to the DNA component of NET and to produce abundant type I IFN, an event that eventually promote further immune system activation.[10] Interestingly, a fraction of SLE patients develop ANCA in addition to autoantibodies against nuclear antigens,[28-31] which allows speculating that NETotic neutrophils may serve as a source of both cytoplasmic and nuclear antigens in this disease. We analyzed spontaneous NETosis in lupus prone lpr/lpr mice and correlated the rate of NETosis with ANCA development. We found that, similarly to the human setting, only a portion of *lpr/lpr* mice developed ANCA and these mice had an increased spontaneous NETosis of naive PMNs. We also tried to correlate ANCA development with

features of autoimmune vasculitis in these same mice and found that, despite the prominent development of a glomerular lupus-like nephritis, mice with the highest ANCA titers clearly showed more conspicuous interstitial vasculitic lesions.

Herein we have extended the correlation between ANCA induction of NETosis and autoimmune vascular damage in human pathology,[12] demonstrating the primary role of NET in pathogenic ANCA induction through mDC cross-presentation in mice. In addition, we corroborated this finding in humans, showing mDCs loaded with MPO and directly interacting with NET structures in skin lesions from patients diagnosed with MPO-ANCA–associated microscopic poliangiitis and SLE. Our study contributes to the idea that NET, although conceived as weapon to defeat extracellular pathogens, may operate hostilely by inducing and fostering autoimmunity.

Acknowledgments

This work was supported by the Italian Association for Cancer Research and the Association for International Cancer Research.

Authorship

Contribution: S.S. and C.T. designed and performed experiments and data analysis and wrote the paper; C. Guarnotta provided histopathology and immunohistochemical expertise; C.C. and C.V. performed FACS analysis; B.C. performed immunohistochemical analysis of mouse tissue; M.P. performed in vivo experiments; P.C. performed confocal microscopy experiments; S.P. contributed to in vitro experiments; C. Guiducci provided critical reagent and reviewed the manuscript; and M.P.C. contributed to study design and data analysis and wrote the paper.

Conflict-of-interest disclosure: C. Guiducci is a full-time employee at Dynavax Technologies Corporation. The remaining authors declare no competing financial interests.

Correspondence: Mario P. Colombo, Molecular Immunology Unit, Department of Experimental Oncology and Molecular Medicine, Fondazione Istituti di Ricovero e Cura a Carattere Scientifico Istituto Nazionale Tumori Via Amadeo 42, 20133 Milano, Italy; e-mail: mario.colombo@istitutotumori.mi.it.

References

1. Nathan C. Neutrophils and immunity: challenges and opportunities. *Nat Rev Immunol.* 2006;6(3):173-182.
2. Di Carlo E, Forni G, Lollini P, Colombo MP, Modesti A, Musiani P. The intriguing role of polymorphonuclear neutrophils in antitumor reactions. *Blood.* 2001;97(2):339-345.
3. Cassatella MA, Locati M, Mantovani A. Never underestimate the power of a neutrophil. *Immunity.* 2009;31(5):698-700.
4. Brinkmann V, Reichard U, Goosmann C, et al. Neutrophil extracellular traps kill bacteria. *Science.* 2004;303(5663):1532-1535.
5. Fuchs TA, Abed U, Goosmann C, et al. Novel cell death program leads to neutrophil extracellular traps. *J Cell Biol.* 2007;176(2):231-241.
6. Remijsen Q, Kuijpers TW, Wirawan E, Lippens S, Vandenabeele P, Vanden Berghe T. Dying for a cause: NETosis, mechanisms behind an antimicrobial cell death modality. *Cell Death Differ.* 2011;18(4):581-588.
7. Alcorta DA, Barnes DA, Dooley MA, et al. Leukocyte gene expression signatures in antineutrophil cytoplasmic autoantibody and lupus glomerulonephritis. *Kidney Int.* 2007;72(7):853-864.
8. Bennett L, Palucka AK, Arce E, et al. Interferon and granulopoiesis signatures in systemic lupus erythematosus blood. *J Exp Med.* 2003;197(6):711-723.
9. Lande R, Ganguly D, Facchinetti V, et al. Neutrophils activate plasmacytoid dendritic cells by releasing self-DNA-peptide complexes in systemic lupus erythematosus. *Sci Transl Med.* 2011;3(73):73ra19.
10. Garcia-Romo GS, Caielli S, Vega B, et al. Netting neutrophils are major inducers of type I IFN production in pediatric systemic lupus erythematosus. *Sci Transl Med.* 2011;3(73):73ra20.
11. Villanueva E, Yalavarthi S, Berthier CC, et al. Netting neutrophils induce endothelial damage, infiltrate tissues, and expose immunostimulatory molecules in systemic lupus erythematosus. *J Immunol.* 2011;187(1):538-552.
12. Kessenbrock K, Krumbholz M, Schonermarck U, et al. Netting neutrophils in autoimmune small-vessel vasculitis. *Nat Med.* 2009;15(6):623-625.
13. Falk RJ, Becker M, Terrell R, Jennette JC. Anti-myeloperoxidase autoantibodies react with native but not denatured myeloperoxidase. *Clin Exp Immunol.* 1992;89(2):274-278.
14. Specks U. What you should know about PR3-ANCA: conformational requirements of proteinase 3 (PR3) for enzymatic activity and recognition by PR3-ANCA. *Arthritis Res.* 2000;2(4):263-267.
15. Colombo MP, Lombardi L, Stoppacciaro A, et al. Granulocyte colony-stimulating factor (G-CSF) gene transduction in murine adenocarcinoma drives neutrophil-mediated tumor inhibition in vivo: neutrophils discriminate between G-CSF-producing and G-CSF-nonproducing tumor cells. *J Immunol.* 1992;149(1):113-119.
16. Ziegler-Heitbrock L, Ancuta P, Crowe S, et al. Nomenclature of monocytes and dendritic cells in blood. *Blood.* 2010;116(16):e74-e80.
17. Sangaletti S, Gioiosa L, Guiducci C, et al. Accelerated dendritic-cell migration and T-cell priming in SPARC-deficient mice. *J Cell Sci.* 2005;118(16):3685-3694.
18. Wernick RM, Smith DL, Houghton DC, et al. Reliability of histologic scoring for lupus nephritis: a community-based evaluation. *Ann Intern Med.* 1993;119(8):805-811.
19. Tripodo C, Gri G, Piccaluga PP, et al. Mast cells and Th17 cells contribute to the lymphoma-associated pro-inflammatory microenvironment of angioimmunoblastic T-cell lymphoma. *Am J Pathol.* 2010;177(2):792-802.
20. Metzler KD, Fuchs TA, Nauseef WM, et al. Myeloperoxidase is required for neutrophil extracellular trap formation: implications for innate immunity. *Blood.* 2011;117(3):953-959.
21. Jarius S, Eichhorn P, Albert MH, et al. Intravenous immunoglobulins contain naturally occurring antibodies that mimic antineutrophil cytoplasmic antibodies and activate neutrophils in a TNFalpha-dependent and Fc-receptor-independent way. *Blood.* 2007;109(10):4376-4382.
22. Martinelli S, Urosevic M, Daryadel A, et al. Induction of genes mediating interferon-dependent extracellular trap formation during neutrophil differentiation. *J Biol Chem.* 2004;279(42):44123-44132.
23. Witko-Sarsat V, Daniel S, Noel LH, Mouthon L. Neutrophils and B lymphocytes in ANCA-associated vasculitis. *APMIS Suppl.* 2009(127):27-31.
24. Clayton AR, Prue RL, Harper L, Drayson MT, Savage CO. Dendritic cell uptake of human apoptotic and necrotic neutrophils inhibits CD40, CD80, and CD86 expression and reduces allogeneic T cell responses: relevance to systemic vasculitis. *Arthritis Rheum.* 2003;48(8):2362-2374.
25. Kantari C, Pederzoli-Ribeil M, Amir-Moazami O, et al. Proteinase 3, the Wegener autoantigen, is externalized during neutrophil apoptosis: evidence for a functional association with phospholipid scramblase 1 and interference with macrophage phagocytosis. *Blood.* 2007;110(12):4086-4095.
26. Munafo DB, Johnson JL, Brzezinska AA, Ellis BA, Wood MR, Catz SD. DNase I inhibits a late phase of reactive oxygen species production in neutrophils. *J Innate Immun.* 2009;1(6):527-542.
27. Patry YC, Trewick DC, Gregoire M, et al. Rats injected with syngenic rat apoptotic neutrophils develop antineutrophil cytoplasmic antibodies. *J Am Soc Nephrol.* 2001;12(8):1764-1768.
28. Chin HJ, Ahn C, Lim CS, et al. Clinical implications of antineutrophil cytoplasmic antibody test in lupus nephritis. *Am J Nephrol.* 2000;20(1):57-63.
29. Spronk PE, Bootsma H, Horst G, et al. Antineutrophil cytoplasmic antibodies in systemic lupus erythematosus. *Br J Rheumatol.* 1996;35(7):625-631.
30. Manolova I, Dancheva M, Halacheva K. Antineutrophil cytoplasmic antibodies in patients with systemic lupus erythematosus: prevalence, antigen specificity, and clinical associations. *Rheumatol Int.* 2001;20(5):197-204.
31. Galeazzi M, Morozzi G, Sebastiani GD, et al. Anti-neutrophil cytoplasmic antibodies in 566 European patients with systemic lupus erythematosus: prevalence, clinical associations and correlation with other autoantibodies. European Concerted Action on the Immunogenetics of SLE. *Clin Exp Rheumatol.* 1998;16(5):541-546.
32. Drenkard C, Villa AR, Reyes E, Abello M, Alarcon-Segovia D. Vasculitis in systemic lupus erythematosus. *Lupus.* 1997;6(3):235-242.
33. Pradhan VD, Badakere SS, Bichile LS, Almeida AF. Anti-neutrophil cytoplasmic antibodies (ANCA) in systemic lupus erythematosus: prevalence, clinical associations and correlation with other autoantibodies. *J Assoc Physicians India.* 2004;52:533-537.
34. Steinman RM. Linking innate to adaptive immunity through dendritic cells. *Novartis Found Symp.* 2006;279:101-109; discussion 109-113.
35. Donnelly S, Roake W, Brown S, et al. Impaired recognition of apoptotic neutrophils by the C1q/calreticulin and CD91 pathway in systemic lupus erythematosus. *Arthritis Rheum.* 2006;54(5):1543-1556.
36. Gaipl US, Sheriff A, Franz S, et al. Inefficient clearance of dying cells and autoreactivity. *Curr Top Microbiol Immunol.* 2006;305:161-176.

37. Potter PK, Cortes-Hernandez J, Quartier P, Botto M, Walport MJ. Lupus-prone mice have an abnormal response to thioglycolate and an impaired clearance of apoptotic cells. *J Immunol.* 2003;170(6):3223-3232.

38. Gilligan HM, Bredy B, Brady HR, et al. Antineutrophil cytoplasmic autoantibodies interact with primary granule constituents on the surface of apoptotic neutrophils in the absence of neutrophil priming. *J Exp Med.* 1996;184(6):2231-2241.

39. Abdgawad M, Pettersson A, Gunnarsson L, et al. Decreased neutrophil apoptosis in quiescent ANCA-associated systemic vasculitis. *PLoS One.* 2012;7(3):e32439.

40. Griffith TS, Ferguson TA. Cell death in the maintenance and abrogation of tolerance: the five Ws of dying cells. *Immunity.* 2011;35(4):456-466.

41. Bianchi ME, Manfredi AA. High-mobility group box 1 (HMGB1) protein at the crossroads between innate and adaptive immunity. *Immunol Rev.* 2007;220:35-46.

42. Guiducci C, Gong M, Xu Z, et al. TLR recognition of self nucleic acids hampers glucocorticoid activity in lupus. *Nature.* 2010;465(7300):937-941.

43. Santiago-Raber ML, Dunand-Sauthier I, Wu T, et al. Critical role of TLR7 in the acceleration of systemic lupus erythematosus in TLR9-deficient mice. *J Autoimmun.* 2010;34(4):339-348.

44. van Timmeren MM, Heeringa P. Pathogenesis of ANCA-associated vasculitis: recent insights from animal models. *Curr Opin Rheumatol.* 2012; 24(1):8-14.

45. van der Geld YM, Stegeman CA, Kallenberg CG. B cell epitope specificity in ANCA-associated vasculitis: does it matter? *Clin Exp Immunol.* 2004; 137(3):451-459.

46. Nagata S, Nagase H, Kawane K, Mukae N, Fukuyama H. Degradation of chromosomal DNA during apoptosis. *Cell Death Differ.* 2003;10(1): 108-116.

47. Dittmar M, Bischofs C, Matheis N, Poppe R, Kahaly GJ. A novel mutation in the DNASE1 gene is related with protein instability and decreased enzyme activity in thyroid autoimmunity. *J Autoimmun.* 2009;32(1):7-13.